Audio Engineering Society

Convention Paper 8122

Presented at the 128th Convention
2010 May 22–25 London, UK

Wave Field Synthesis using Fractional Order Systems and Fractional Delays

César D. Salvador[1]

[1] Universidad de San Martín de Porres, ISONAR, Surquillo, Lima 34, Peru
csalvador@comunicaciones.usmp.edu.pe

ABSTRACT

A discretization of the generalized 2.5D wave field synthesis driving functions is proposed in this paper. Time discretization is applied with special attention to prefiltering that involves half-order systems and to delaying that involves fractional-sample delays. Space discretization uses uniformly distributed loudspeakers along arbitrarily shaped contours. Visual and numerical comparisons between continuous and discrete synthesis with line, square and circular arrays are shown. An immersive soundscape composed of nature sounds is reported as example. Simulations have been done with MATLAB and real-time reproduction with Pure Data. Simulations of synthesized plane and spherical wave fields, in the whole listening area, report a percentage discretization error of less than 1%, using a 5th order IIR filter for prefiltering and a 3rd order IIR filter per channel for fractional delaying.

1. INTRODUCTION

Wave field synthesis (WFS) is a sound reproduction technique whose theoretical framework was initially formulated by Berkhout et al. [1], [2]. WFS is actually emerging as an optimal format for spatialization of virtual auditory scenes that look for immerse a listener in an almost real acoustic environment, synthesizing wave fronts with physical methods and rendering them through loudspeaker arrays. WFS allows to synthesize virtual acoustical environments by rendering room impulse responses with plane wave fronts, as well as to synthesize virtual sources that appear to emanate from a defined position by rendering them with spherical wave fronts. Thus, it provides the listener with consistent spatial localization cues over large listening areas, using a high number of loudspeakers which in this context are called secondary sources [3].

Although the most widespread application of WFS is the mentioned above, the motivation of this work arise in the composition of immersive soundscapes. The concept of soundscape refers to both the natural acoustic environment and the sounds created by people. The study of soundscape is the subject of acoustic ecology and its main field method is the recording and classification of sounds according to its quality and social significance. Actually, the soundscape and sound art community have special attention on WFS due to its capability to recreate the original recording scene. Since

a background sound is perceived as coming from a non-localized source and a foreground sound as coming from a localized source, their reproduction models can naturally be done with plane and spherical waves, respectively.

In practical WFS applications, it is necessary to compute prefiltering, filtering, delaying and scaling operations on the audio signal to be spatialized before it drives each loudspeaker. These operations form the loudspeaker driving function and, except for prefiltering, they usually need to be computed in real time, according to the position of each secondary source and the actual position (spherical wave) or direction of propagation (plane wave) of the virtual source. Due to most of the real time DSP programming environments include zero-pole filters in their libraries; the main purpose of this document is to provide a discrete-time version of the loudspeaker driving functions in terms of IIR filters.

This paper is organized as follows: Section 2 briefly introduces the continuous wave field synthesis for arbitrary shaped contours. Section 3 proposes a discretization of the continuous driving functions with special attention on prefiltering and delaying stages. Section 4 presents the simulations of the sound pressure fields synthesized with both the continuous and discrete driving functions, as well as the corresponding discretization errors. Section 5 presents the application to the composition of immersive soundscapes, which was the motivation for the present work. Section 6 resumes the goals of the present work as well as the conclusions and ongoing work.

2. CONTINUOUS WAVE FIELD SYNTHESIS

The geometry used in the WFS theory revisited by Spors et al. in [4] is illustrated in figure 1. According to it, the wave field emanating from the virtual source at $\mathbf{x}_s = [\mathrm{x}_s \ \mathrm{y}_s]^\mathrm{T}$ can be synthesized in the listening area enclosed by an arbitrarily shaped contour ∂V using loudspeakers at $\mathbf{x}_0 = [\mathrm{x}_0 \ \mathrm{y}_0]^\mathrm{T}$ along this contour as secondary monopole sources. The normal vector to ∂V at $\mathbf{x}_0$ is the column $\mathbf{n}(\mathrm{x}_0)$ and the reference position is $\mathbf{x}_{\mathrm{ref}} = [\mathrm{x}_{\mathrm{ref}} \ \mathrm{y}_{\mathrm{ref}}]^\mathrm{T}$.

The sound pressure $P(\mathbf{x}, \omega)$ inside the listening area can be expressed by the secondary source driving functions $D(\mathbf{x}_0, \omega)$ and the Green's functions of the monopoles at the boundary ∂V as the Kirchoff-Helmholtz integral

$$P(\mathbf{x}, \omega) = -\frac{1}{4\pi} \oint_{\partial V} D(\mathbf{x}_0, \omega) \frac{e^{-j\frac{\omega}{c}|\mathbf{x_0}-\mathbf{x}_s|}}{|\mathbf{x_0}-\mathbf{x}_s|} dS_0. \qquad (1)$$

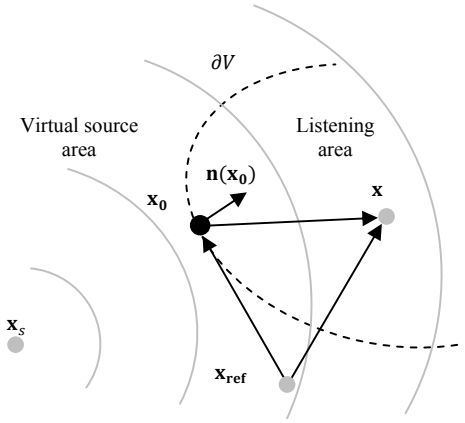

Figure 1: The geometry used in wave field synthesis.

The 2.5D driving function of a loudspeaker at $\mathbf{x_0}$, for the synthesis of a plane wave with spectrum $S_p(\omega)$, $S_P(\mathbf{x}, \omega) = S_p(\omega)\exp(-j\omega\mathbf{n}_p^T\mathbf{x}/c)$, propagating in the $\mathbf{n}_p$ direction, is

$$D_p(\mathbf{x_0}, \omega) = -2a_p(\mathbf{x_0})\sqrt{2\pi|\mathbf{x}_{\mathrm{ref}} - \mathbf{x}_0|}\mathbf{n}_p^\mathrm{T}\mathbf{n}(\mathbf{x}_0)$$
$$\times \frac{1}{\sqrt{c}}(j\omega)^{1/2} e^{-j\omega\frac{\mathbf{n}_p^T\mathbf{x}_0}{c}} S_p(\omega), \qquad (2)$$

where, $|\cdot|$ denotes the Euclidian norm, c the velocity of sound in air, and the selection loudspeaker functions is

$$a_p(\mathbf{x_0}) = \begin{cases} 1 & \text{, if } \mathbf{n}_p^T\mathbf{n}(\mathbf{x_0}) > 0, \\ 0 & \text{, otherwise.} \end{cases} \qquad (3)$$

The 2.5D driving function of a loudspeaker at $\mathbf{x_0}$, for the synthesis of the non focused spherical wave $S_s(\mathbf{x}, \omega) = S_s(\omega)\exp(-j\omega|\mathbf{x} - \mathbf{x}_s|/c)/|\mathbf{x} - \mathbf{x}_s|$, with spectrum $S_s(\omega)$ emanating from $\mathbf{x}_s$, is

$$D_s(\mathbf{x_0}, \omega) = -2a_s(\mathbf{x_0})\sqrt{2\pi|\mathbf{x_{ref}} - \mathbf{x_0}|}\frac{(\mathbf{x_0} - \mathbf{x}_s)^T\mathbf{n}(\mathbf{x_0})}{|\mathbf{x_0} - \mathbf{x}_s|^2}$$
$$\times \frac{1}{\sqrt{c}}\left(j\omega + \frac{c}{|\mathbf{x_0}-\mathbf{x}_s|}\right)(j\omega)^{-1/2} e^{-j\omega\frac{|\mathbf{x_0}-\mathbf{x}_s|}{c}} S_s(\omega), \qquad (4)$$

where the loudspeaker selection function is:

$$a_s(\mathbf{x_0}) = \begin{cases} 1 & \text{, if } (\mathbf{x_0} - \mathbf{x}_s)^T\mathbf{n}(\mathbf{x_0}) > 0, \\ 0 & \text{, otherwise.} \end{cases} \qquad (5)$$

The rendering of sources positioned in between the loudspeakers and the listener, called focused sources, can be derived using a complex conjugate version of equation (1). This is possible thanks to the time-reversal invariance of the wave equation: for each burst of sound diverging from a source, there exists a set of waves that retraces its paths and converges simultaneously at the original source site as if time were running backwards [5], [6]. Here, it is used a modified version of the driving functions proposed in [7] and [8]:

$$D_{fs}(\mathbf{x_0},\omega)=\sqrt{\frac{|\mathbf{x_{ref}}-\mathbf{x_0}|}{|\mathbf{x_{ref}}-\mathbf{x_0}|+|\mathbf{x_0}-\mathbf{x}_s|}}\frac{(\mathbf{x_0}-\mathbf{x}_s)^T\mathbf{n}(\mathbf{x_0})}{|\mathbf{x_0}-\mathbf{x}_s|^{3/2}} \times\frac{-\mathrm{j}}{\sqrt{2\pi c}}(j\omega)^{1/2}e^{j\omega\frac{|\mathbf{x_0}-\mathbf{x}_s|}{c}}\hat{S}_s(\omega). \quad (6)$$

The next section deals with discretization of the revisited WFS reproduction model. Space discretization is mainly done on equation (1) and time discretization on equations (2), (4) and (6).

3. DISCRETE WAVE FIELD SYNTHESIS

3.1. Space discretization

Although the theory presented assumes a spatial continuous distribution of secondary sources, practical implementations of WFS will consist of secondary sources that are placed at spatially discrete positions [4]. Let suppose that discrete-time driving functions $D(\mathbf{x}_0,z)$ have already been obtained at a sample rate f_s. When a finite set of loudspeakers are uniformly distributed along the arbitrarily shaped contour ∂V, the discrete space formulation of equation (1), for continuous and discrete time, are stated as follows:

$$P_{cont-time}(\mathbf{x},\omega)=-\frac{\Delta\mathbf{x_0}}{4\pi}\sum_{l=0}^{L}D(\mathbf{x}_{0,l},\omega)\frac{e^{-j\omega\frac{|\mathbf{x}-\mathbf{x}_{0,l}|}{c}}}{|\mathbf{x}-\mathbf{x}_{0,l}|}, \quad (7)$$

$$P_{disc-time}(\mathbf{x},z)=-\frac{\Delta\mathbf{x_0}}{4\pi}\sum_{l=0}^{L}D(\mathbf{x}_{0,l},z)\frac{z^{-f_s\frac{|\mathbf{x}-\mathbf{x}_{0,l}|}{c}}}{|\mathbf{x}-\mathbf{x}_{0,l}|}, \quad (8)$$

where $\mathbf{x}_{0,l}$ is the position of the lth loudspeaker and $\Delta\mathbf{x_0}$ is the distance between two adjacent loudspeakers that defines the spatial aliasing frequency $\mathrm{f_a}=\mathrm{c}/\Delta\mathrm{x}_0$. Incoming simulations of sound pressure fields inside the listening area in section 4, with contours chosen to be line, square and circular arrays, are calculated with these equations. They will allow for visual comparisons on the following discrete time version of continuous driving functions. All percentage errors between continuous and discrete-time wave field synthesis have been computed using:

$$e_r(P_1,P_2)=\frac{|P_1-P_2|_\infty}{|P_1|_\infty}\times 100\%, \quad (9)$$

where $|\cdot|_\infty$ denotes the L^∞ norm.

3.2. Time discretization

A discretization in time of 2.5D WFS driving functions for the rendering of plane, focused spherical and non-focused spherical waves, using monopole secondary sources, requires special attention to the prefiltering and delaying stages. The pre-filter stage $(j\omega)^\alpha$ involves half-order systems as a consequence of using the asymptotic expansion of the Hankel function for large arguments in the 2D Green function [9], which allows to use a scaled version of the 3D Green function. The time-delay stage involves fractional sample delays due to rational multiples of the sample time.

On the following, two continuous to discrete mappings will be used, both at a sampling rate f_s. As filters and prefilters are represented by rational functions, the following Al-alaoui approximation is used on them

$$j\omega\approx\frac{8f_s}{7}\frac{1-z^{-1}}{1+\frac{1}{7}z^{-1}}, \quad (10)$$

which corresponds to an interpolation between the Euler and Tustin approximations [10], [11]. As continuous delays appears as exponential functions, the following standard mapping is used on them

$$\mathrm{z}=\exp(j\omega/f_s). \quad (11)$$

In both cases of prefilters and delays, the objective is to find rational functions of z which can be programmed as IIR or FIR filters. Next section starts with the discretization of the one-zero filter in equation (4) and follows with the discretization of fractional prefilters and fractional delay.

3.2.1. The filter for non-focused spherical wave

The Al-alaoui approximation in (10) of the variable zero $(j\omega+c/|\mathbf{x_0}-\mathbf{x}_s|)$ in the non-focused spherical wave driving function of equation (4) leads to:

$$F(z) = \left(\frac{8f_s}{7} + \frac{c}{|\mathbf{x_0}-\mathbf{x}_s|}\right) \frac{1 - \frac{|\mathbf{x_0}-\mathbf{x}_s| - \frac{c}{8f_s}}{7c} z^{-1}}{1 + \frac{1}{7} z^{-1}}. \quad (12)$$

3.2.2. Fractional order prefilters

The factor $(j\omega)^{0.5}$ on equations (2) and (6) shows that the rendering of plane and focused spherical waves requires half order differentiation. The factor $(j\omega)^{-0.5}$ on equation (4) shows that the rendering of non-focused spherical waves requires half order integration. The continuous to discrete Al-alaoui approximation of $(j\omega)^{\alpha}$, using equation (10) at a sampling rate f_s, can be expanded into a power series as follows

$$(j\omega)^{\alpha} \approx \left(\frac{8f_s}{7}\frac{1 - z^{-1}}{1 + \frac{1}{7}z^{-1}}\right)^{\alpha} \approx \sum_{k=0}^{K} h_k z^{-k}. \quad (13)$$

Following the Grünwald-Letnikov approach for fractional integration and differentiation [12], we can compute the Taylor series of the middle term. The coefficients of the $K+1$ order polynomial in z now is

$$h_k = \left(\frac{8f_s}{7}\right)^{\alpha} \sum_{j=0}^{k} (-1)^j \left(\frac{1}{7}\right)^{k-j} \binom{\alpha}{j} \binom{-\alpha}{k-j} \quad (14)$$

where $\binom{\alpha}{j} = \frac{\Gamma(\alpha+1)}{\Gamma(j+1)\Gamma(\alpha-j+1)}$ is the generalization of the binomial function for rational numbers, and $\Gamma(\alpha) = \int_0^{\infty} t^{\alpha-1} e^{-t} dt$ is the gamma function: an interpolation that extents the factorial function to rational numbers. Since the later polynomial representation corresponds to a very large FIR filter, it is preferable to transform it into a short IIR filter as follows:

$$(j\omega)^{\alpha} \approx \sum_{k=0}^{K} h_k z^{-k} = \frac{\sum_{k=0}^{m} b_k z^{-k}}{1 + \sum_{k=1}^{n} a_k z^{-k}} = g\frac{(1-\zeta_1 z^{-1})(1-\zeta_2 z^{-1}) \dots (1-\zeta_m z^{-1})}{(1-\pi_1 z^{-1})(1-\pi_2 z^{-1}) \dots (1-\pi_n z^{-1})}. \quad (15)$$

To compute the numerator and denominator from h_k the Shank's method for least squares approximation is used according to [13] and [14]. The idea is to interpret b_k as the convolution product $(h * a)_k$. Once its associated Toeplitz matrix is identified, its lower half matrix is taken. Then $\mathbf{a} = [a_1 \quad a_2 \quad \dots \quad a_n]^{\mathbf{T}}$ is first computed from $\mathbf{h_2} = [h_{m+1} \quad h_{m+2} \quad \dots \quad h_{N-1}]^{\mathbf{T}}$, with the following pseudo inverse matrix:

$$\mathbf{a} = -\left(\mathbf{H}_2^T \mathbf{H}_2\right)^{-1} \mathbf{H}_2^T \mathbf{h}_2, \quad (16)$$

where

$$\mathbf{H_2} = \begin{bmatrix} h_m & h_{m-1} & \cdots & h_{m-n+1} \\ h_{m+1} & h_m & \dots & h_{m-n+2} \\ \vdots & \vdots & \ddots & \vdots \\ h_{N-2} & h_{N-3} & \dots & h_{N-n-1} \end{bmatrix}.$$

The next step is to compute the impulse response of the filter $1/(1 + \sum_{k=1}^{n} a_k z^{-k})$, denoted $g_k = \delta_k - \sum_{l=1}^{n} a_l g_{k-l}$, $k = 0,1, \dots, N-1$. With this impulse response, a new pseudo inverse matrix appears to compute $\mathbf{b} = [b_0 \quad b_1 \quad \dots \quad b_m]^{\mathbf{T}}$ from $\mathbf{h} = [h_0 \quad h_1 \quad \dots \quad h_{N-1}]^{\mathbf{T}}$ as follows:

$$\mathbf{b} = (\mathbf{G}^{\mathbf{T}}\mathbf{G})^{-1}\mathbf{G}^{\mathbf{T}}\mathbf{h}, \quad (17)$$

where

$$\mathbf{G} = \begin{bmatrix} g_0 & 0 & \cdots & 0 \\ g_1 & g_0 & \dots & 0 \\ \vdots & \vdots & \ddots & \vdots \\ g_{N-1} & g_{N-2} & \dots & g_{N-m-1} \end{bmatrix}.$$

Equations (14), (16) and (17) allows to compute the half order prefilters using $\alpha = 0.5$ for plane and focused spherical waves and $\alpha = -0.5$ for non focused spherical waves. Thus, prefilters can be expressed as

$$P_{\alpha}(z) = g\frac{(1-\zeta_1 z^{-1})(1-\zeta_2 z^{-1}) \dots (1-\zeta_m z^{-1})}{(1-\pi_1 z^{-1})(1-\pi_2 z^{-1}) \dots (1-\pi_n z^{-1})} \quad (18)$$

Next section deals with fractional delays.

3.2.3. Fractional delays

The ideal impulse response of a fractional delay $z^{-\tau}$, where τ is a real number is $b_k = \sin(\pi[k-\tau])/\pi[k-\tau]$, for all k. When the desired delay τ assumes an integer value, the impulse response reduces to $\delta_{k-\tau}$. Several FIR and IIR filters for approximating this ideal impulse response have been reviewed by Laakso et al. in [15], [16], from where it has been chosen two methods: FIR Lagrange interpolation and IIR Tiran all pass filtering, due to their good behavior at low frequencies in terms of magnitude and phase delay accuracy.

In both approaches, the total delay τ is separated into an integer delay z^{-M} and a non-integer delay $T_{\tau-M}(z)$, such that it can be implemented with a shift operator followed by a FIR filter or an IIR filter. Let the order of the filter be equal to q, then the optimum choice for the integer delay M is given by

$$M = \begin{cases} round(\tau) - \dfrac{q}{2} & for\ even\ q \\ floor(\tau) - \dfrac{q-1}{2} & for\ ood\ q \end{cases} \quad (19)$$

which is appropriate for arbitrarily long delays as it happens in WFS. The objective, in general, is to express the total delay as

$$z^{-M} T_{\tau-M}(z) = z^{-M} \frac{b_0 + b_1 z^{-1} + \cdots + b_q z^{-q}}{a_0 + a_1 z^{-1} + \cdots + a_q z^{-q}} \quad (20)$$

The coefficients of the FIR Lagrange interpolating filter that implements the non-integer delay $T_{\tau-M}(z)$ are

$$b_{k-M} = \prod_{\substack{i=M \\ i \neq k}}^{M+q} \frac{\tau - i}{k - i} \quad (21)$$

where $k = M,\ M+1,\ \ldots,\ M+q$, τ can also be integer, and $a_k = \delta_k$.

The coefficients of the IIR Tiran all-pass filter that implements the non-integer delay $T_{\tau-M}(z)$ are

$$a_k = \begin{cases} (-1)^k \binom{q}{k} \prod_{i=0}^{q} \dfrac{\tau - M - q + i}{\tau - M - q + k + i}, & \tau \notin \mathbb{Z} \\ \delta_k & \tau \in \mathbb{Z} \end{cases} \quad (22)$$

and

$$b_k = \begin{cases} a_{q-k}, & \tau \notin \mathbb{Z} \\ \delta_{k-(\tau-M)} & \tau \in \mathbb{Z} \end{cases} \quad (23)$$

where $k = 0,1,\ldots,q$.

Up to here, all the frequency dependent stages in the 2.5D WFS driving functions have been discretisized. Next section resumes these results.

3.3. Discrete 2.5D driving functions

In practice, filtering F, delaying $z^{-M}T_{\tau-M}$ and scaling A operations need to be applied in real-time to audio samples in order to produce each loudspeaker's driving function, according to the distance $|\mathbf{x_0} - \mathbf{x}_s|$ between the virtual source and the loudspeaker in case of spherical model, or according to the direction of propagation $\mathbf{n}_p^T\mathbf{x_0}$ in case of plane waves. An additional prefiltering operation P_α independent of position is also required and it can be computed only once for all the loudspeakers. After an appropriate ordering of factors, a discrete version of the 2.5D driving functions for plane, non-focused spherical and focused spherical waves appears respectively in equations (24), (26) and (29), which is preferable to state in gain-zero-pole form, due to that most of real time DSP environments include zero-pole filters.

The discrete driving function of a loudspeaker at $\mathbf{x_0}$ for the synthesis of an audio source with spectrum S using a plane model propagating in the $\mathbf{n}_p$ direction is

$$D_p = z^{-M} T_{\tau-M} A P_\alpha S, \quad (24)$$

where P_α is computed with (14), (16) and (17) for $\alpha = 0.5$,

$$A = -2a_p(\mathbf{x_0}) \sqrt{\frac{2\pi|\mathbf{x_{ref}} - \mathbf{x_0}|}{c}}\, \mathbf{n}_p^T \mathbf{n}(\mathbf{x_0}), \quad (25)$$

M is computed with (19), and $T_{\tau-M}$ is computed with (21), or (22) and (23), for $\tau = f_s\ \mathbf{n}_{\mathrm{PW}}^T \mathbf{x_0}/c$.

The discrete driving function of a loudspeaker at $\mathbf{x_0}$ for the synthesis of an audio source with spectrum S using a non focused spherical model emanating from $\mathbf{x}_s$ is

$$D_S = z^{-M} T_{\tau-M} A F P_\alpha S, \quad (26)$$

where P_α is computed with (14), (16) and (17) for $\alpha = -0.5$,

$$F = \left(\frac{8f_s}{7} + \frac{c}{|\mathbf{x_0} - \mathbf{x}_s|}\right) \frac{1 - \frac{|\mathbf{x_0} - \mathbf{x}_s| - \frac{c}{8f_s}}{|\mathbf{x_0} - \mathbf{x}_s| + \frac{7c}{8f_s}} z^{-1}}{1 + \frac{1}{7} z^{-1}}, \quad (27)$$

$$A = -2a_s(\mathbf{x_0}) \sqrt{\frac{2\pi|\mathbf{x_{ref}} - \mathbf{x_0}|}{c}}\, \frac{(\mathbf{x_0} - \mathbf{x}_s)^T \mathbf{n}(\mathbf{x_0})}{|\mathbf{x_0} - \mathbf{x}_s|^2}, \quad (28)$$

M is computed with (19) and $T_{\tau-M}$ is computed with (21), or (22) and (23), for $\tau = f_s\ |\mathbf{x_0} - \mathbf{x}_s|/c$.

The discrete driving function of a loudspeaker at $\mathbf{x_0}$ for the synthesis of an audio source with spectrum S using a focused spherical model emanating from $\mathbf{x}_s$ is

$$D_{fS} = z^{M} T_{\tau-M}^{*} A P_\alpha S, \quad (29)$$

where P_α is computed with (14), (16) and (17) for $\alpha = 0.5$,

$$A = \frac{-\mathrm{j}}{\sqrt{2\pi c}} \sqrt{\frac{|\mathbf{x_{ref}} - \mathbf{x_0}|}{|\mathbf{x_{ref}} - \mathbf{x_0}| + |\mathbf{x}_s - \mathbf{x_0}|}}\, \frac{(\mathbf{x_0} - \mathbf{x}_s)^T \mathbf{n}(\mathbf{x_0})}{|\mathbf{x_0} - \mathbf{x}_s|^{3/2}} \quad (30)$$

M is computed with (19), and $T^*_{\tau-M}$ is computed with (21), or (22) and (23), for $\tau = f_s\,|\mathbf{x_0} - \mathbf{x}_s|/c$. Here, $*$ denotes the complex conjugate operator.

In the next section, the sound pressure fields in the whole listening area are synthesized using the continuous and discrete driving functions.

4. SIMULATIONS OF SOUND PRESSURE FIELDS

Figures 4 to 7 allow for visual comparisons of sound pressure fields synthesized from continuous and discrete driving functions. Percentage discretization errors are also shown for real, magnitude and phase components of these complex fields. Sound pressure fields are computed with real part of equations (7) and (8), and percentage errors with equation (9).

In order to select suitable parameters for simulations, it has previously been evaluated the discretization error for different orders of both prefiltering and delaying stages. These results are shown in figures 2 and 3, from where it can be seen that a 5th order prefilter provides the best result, and it is enough to compute the fractional delays with 1st, 2nd or 3rd order filters on either a FIR or IIR approach. On incoming simulations, the following discretization parameters for prefilters in equations (14), (16) and (17) have been chosen: $K = 150$, $m = n = 6$ and $N = 25$. They return the half differentiator (Table 1) and the half integrator (Table 2) used as prefilter in (10) and (11).

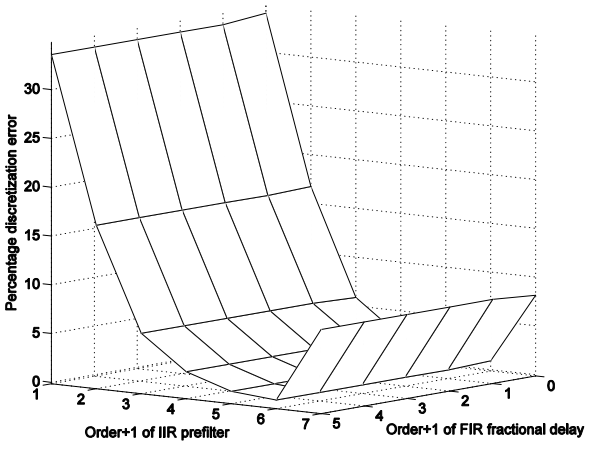

Figure2. Discretization errors for different orders of IIR prefilters and FIR fractional delays.

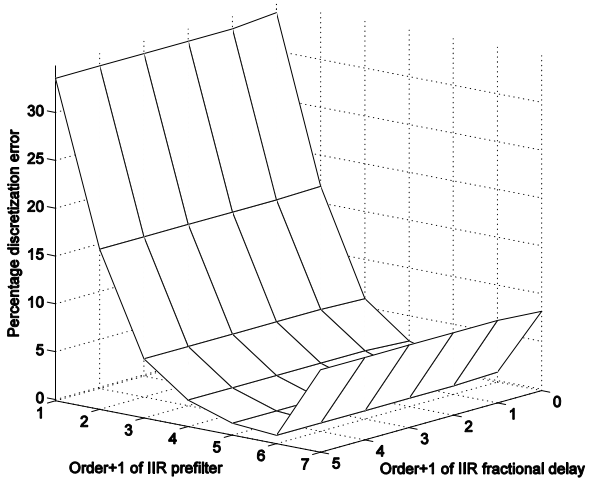

Figure3. Discretization errors for different orders of IIR fractional prefilters and IIR fractional delays.

Gain g	224.4994					
Zeros ζ_k	0.9887	0.8972	0.7112	0.4478	0.1628	-0.0590
Poles π_k	0.9547	0.8158	0.5867	0.3029	-0.1214	0.0386

Table1. Prefilter P_{PW} for the synthesis of plane and focused spherical waves ($\alpha = 0.5$).

Gain g	0.0045					
Zeros ζ_k	0.9887	0.8972	0.7112	0.4478	0.1628	-0.0590
Poles π_k	0.9547	0.8158	0.5867	0.3029	-0.1214	0.0386

Table2. Prefilter P_{SW} for the synthesis of non focused spherical waves ($\alpha = -0.5$).

For the fractional delay it has been chosen the Tiran all pass filters of order $q=3$. In the following figures 4 to 7, the sound pressure fields synthesized with continuous driving functions (left) and with discrete driving functions (left) are shown for different wave fronts and different loudspeakers distributions. In all cases, the source is a 500Hz pure tone.

Figure 4 shows a plane wave field synthesized with a line array of 16 loudspeakers. The plane wave direction is -90° and the center of the line array is (0,3m). The distance between loudspeakers $\Delta\mathbf{x_0}$ is 26.67cm. The spatial aliasing frequency f_a is 1275Hz.

Figure 5 shows a plane wave field synthesized with a circular array of 48 loudspeakers. The plane wave direction is -45° and the radius of curvature of the array

is 3.75m. The distance between loudspeakers $\Delta\mathbf{x_0}$ is 23.40cm. The spatial aliasing frequency f_a is 1452Hz.

Figure 6 shows a non-focused spherical wave field synthesized with a square array with 48 loudspeakers. The spherical wave center is (-3m,3m). The distance between loudspeakers $\Delta\mathbf{x_0}$ is 26.67cm. The spatial aliasing frequency f_a is 1275Hz.

Figure 7 shows a focused spherical wave field synthesized with a circular array with 48 loudspeakers. The center of the spherical wave is (0,1m). The distance between loudspeakers $\Delta\mathbf{x_0}$ is 26.67cm. The spatial aliasing frequency f_a is 1275Hz.

P_1	P_2	$e_r(P_1, P_2)$
Re (P_{cont})	Re (P_{disc})	00.8177%
mag (P_{cont})	mag (P_{disc})	00.7306%
phase (P_{cont})	phase (P_{disc})	11.0708%

Table3. Percentage discretization errors for Figure 4.

P_1	P_2	$e_r(P_1, P_2)$
Re (P_{cont})	Re (P_{disc})	1.1434%
mag (P_{cont})	mag (P_{disc})	0.7306%
phase (P_{cont})	phase (P_{disc})	3.0430%

Table4. Percentage discretization errors for Figure 5.

P_1	P_2	$e_r(P_1, P_2)$
Re (P_{cont})	Re (P_{disc})	0.7406%
mag (P_{cont})	mag (P_{disc})	0.0386%
phase (P_{cont})	phase (P_{disc})	2.9114%

Table5. Percentage discretization errors for Figure 6.

P_1	P_2	$e_r(P_1, P_2)$
Re (P_{cont})	Re (P_{disc})	0.7579%
mag (P_{cont})	mag (P_{disc})	0.7306%
phase (P_{cont})	phase (P_{disc})	7.7404%

Table6. Percentage discretization errors for Figure 7.

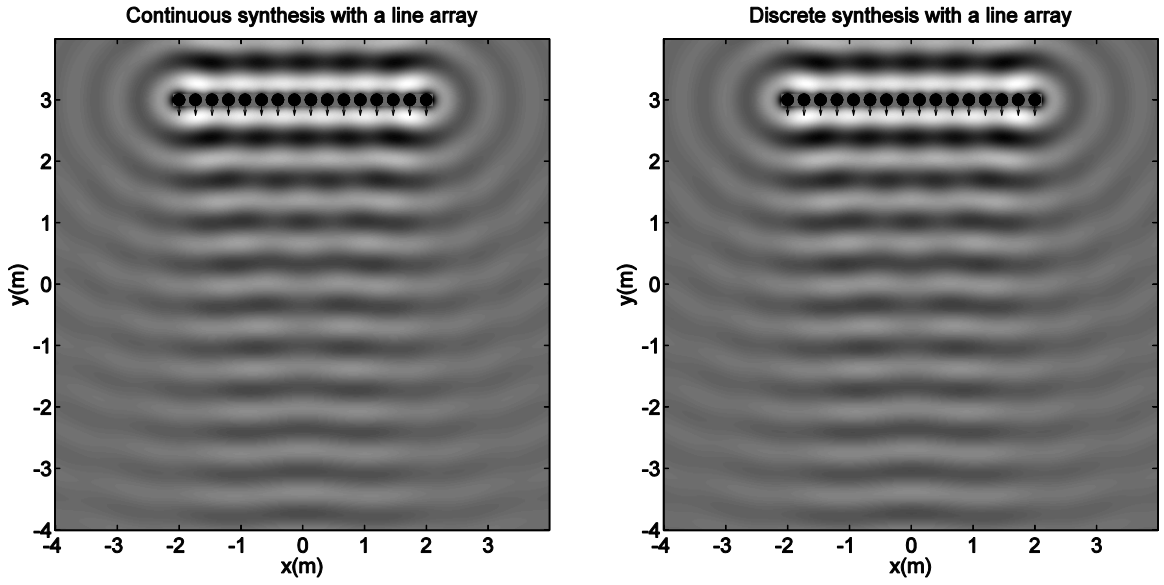

Figure4. A plane wave field synthesized with a line array of 16 loudspeakers.

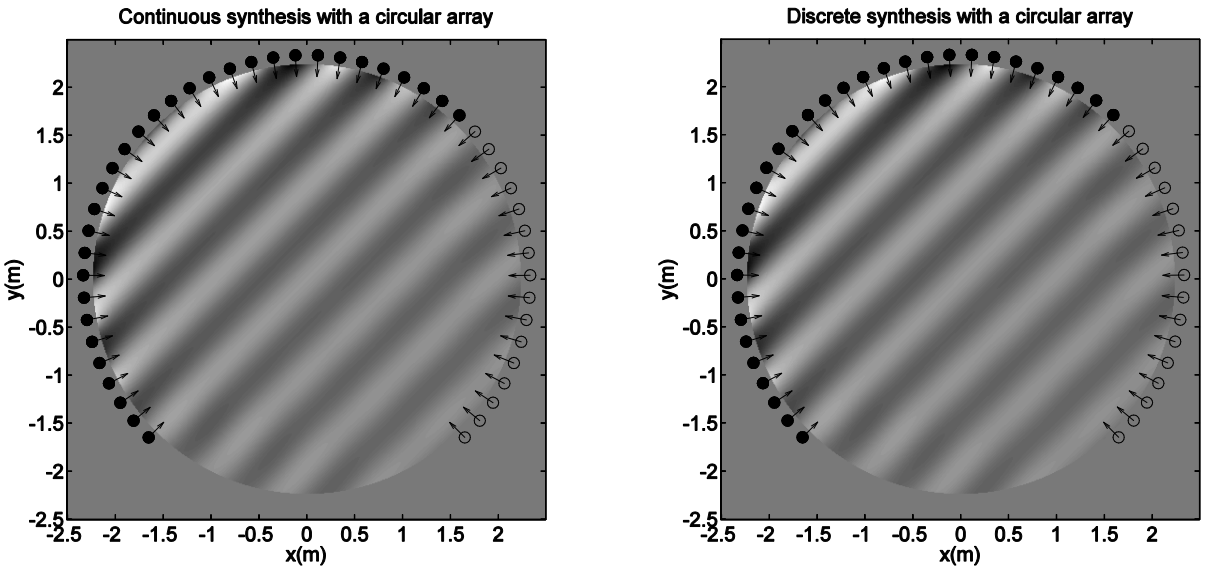

Figure5. A plane wave field synthesized with a circular array of 48 loudspeakers.

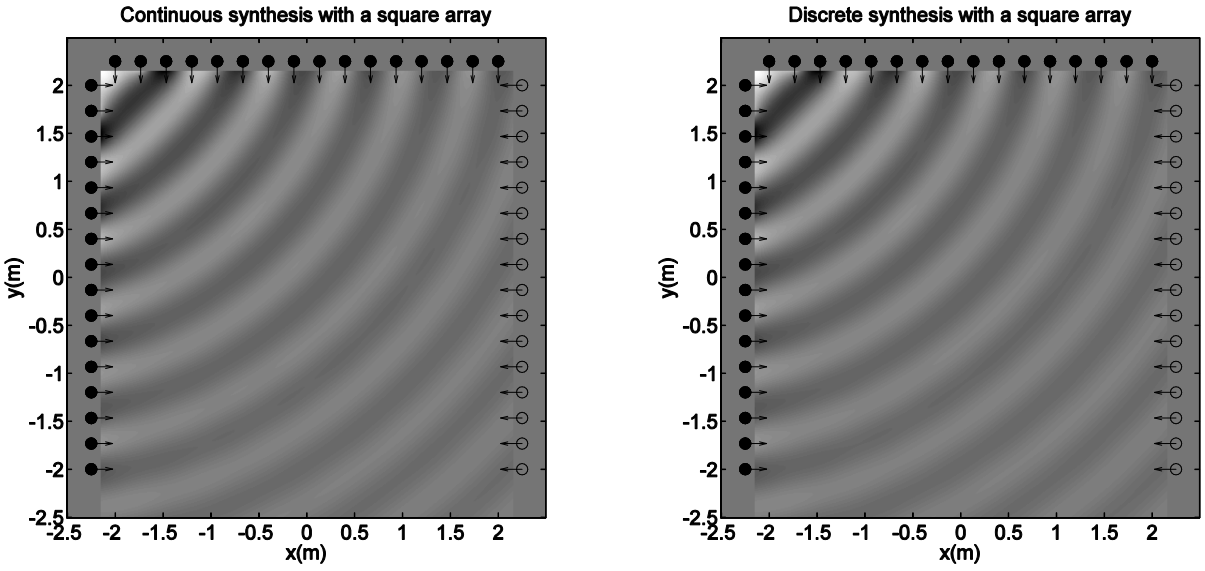

Figure6. A non-focused spherical wave field synthesized with a square array of 48 loudspeakers.

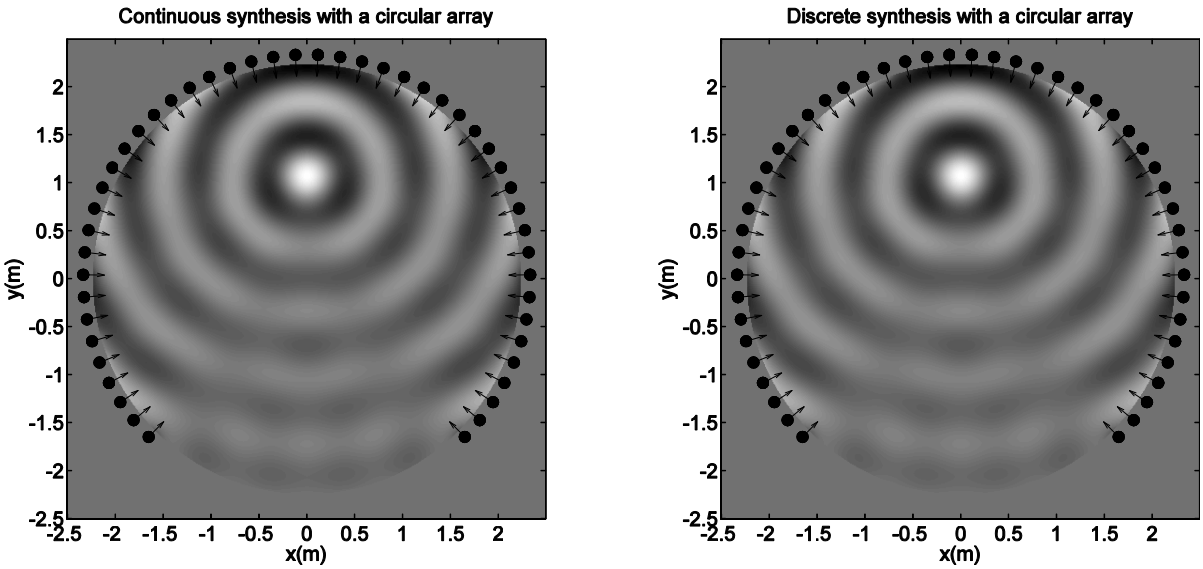

Figure7. A focused spherical wave field synthesized with a circular array of 48 loudspeakers.

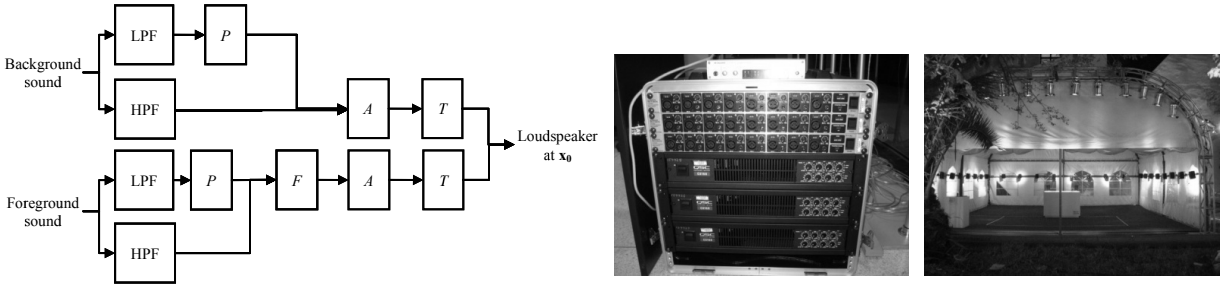

(a) (b) (c)

Figure8. The system for the auralization of natural sounds is composed of: a) The real-time driving function computations for each loudspeaker, b) the audio interface between computer and loudspeakers and c) the virtual auditory scene with 24 loudspeakers that defines a 6x6m listening area.

5. AN APPLICATION TO IMMERSIVE SOUNDSCAPES

This section returns to the concept of soundscape. Although the reproduction of sound using spherical and plane wave models is widely used in room acoustics (spherical waves are used for rendering of audio tracks such as music and speech, while plane waves are used for the rendering of room impulse responses, reproducing in that way the acoustics of a different room), it is proposed here another less known application for the composition and recreation of soundscapes. Since background sound are perceived as coming from a non-localized source and a foreground sound as from a localized source, their reproduction model appear in a natural respectively with plane and spherical wave models. Within this framework this paper reports, as example of the proposed discrete scheme, a practical auralization of an immersive soundscape composed with natural sounds recorded in

the highlands and beaches of Lima, Peru. Next section explains the considerations for data registration.

5.1. Data registration

Monaural samples, recorded with omnidirectional and wind-shielded microphones, should be used with this reproduction scheme. It is preferable the use of a digital recorder with 24 quantization and capable of capturing at least 44100 samples per second. It is also strongly recommended to normalize the samples at -3dB and then to eliminate the DC offset. For the following application, audio samples have been recorded using digital recorders such that the Sound Device 722 and the Sony PCMD50, both with an external, omnidirectional and wind-screened microphone.

Once the collection of samples has been recorded, a spectral representation of the sound objects should be done. This representation is very helpful to classify them in background and foreground sounds. For example, the spectrograms of a background sound such that the wind blowing through the trees have a smooth covering of all almost the whole time-frequency domain. This is not the case for example for the foreground sound of the song of a bird, whose spectrograms are composed of several increasing and decreasing curved lines referring to the fundamental and harmonic frequencies.

5.2. Auralization of nature sounds

The multichannel auralization has been implemented using Pure Data [17], with a graphical interface that allows the composer to render up to five virtual sources over a 6mx6m listening area through 24 audio channels, giving the spectator the sensation of being immerse in a natural scene due to the spatial component added to the piece of art. The equipment used for this purpose was: one Mac Book Pro laptop, one M-audio Profire Lightbridge audio interface, three Behringer ADA8000 digital to analog converters, three QSC168X eight channel amplifiers, and 24 Behringer 1CBK loudspeakers.

Figure 8 presents a practical implementation of an immersive soundscape composed with natural sounds recorded in the highlands and beaches of Lima, Peru. A real system was developed in ISONAR Sound Research Workshop, at University of San Martin de Porres. It was presented for the first time in September 2009, during the "II Festival Lima Sonora", as part of a bigger event called "La semana del arte en Buenos Aires" [18].

6. CONCLUSION

A discretization of the Wave Field Synthesis method has been proposed, with special attention on prefiltering and delaying stages. On prefiltering, the following methods has been used: Al-alaoui discretization that corresponds to an interpolation between the Euler and Tustin approximations, the Grünwald-Letnikov approach for fractional integration and differentiation that allows a binomial expansion of the Al-alaoui map whose result is a large FIR filter, and the Shank's least squares approximation method to transform the previous FIR filter into a short IIR one that generates the corresponding half order system. On delaying, the Lagrange interpolation and the Tiran all-pass filtering approaches has been employed to compute respectively the FIR and IIR filters that generate the fractional sample delays.

Simulations illustrated that the discretization of prefiltering directly affects to discretization errors, where the best choice was a 5^{th} order filter (length = 6). On the other hand, the discretization of fractional delays does not significantly affect to discretization errors, where 1^{st}, 2^{nd} or 3^{rd} order FIR or IIR filters are enough. It is important to mention here that large phase errors obtained by simulations are due to discontinuities in the unwrapped phase used for computations, for that reason it is preferable to read the real and magnitude errors. Simulations show a deviation from the continuous formulation of less than 1%. As a practical example, it has been reported the composition of an immersive soundscape composed of nature sounds.

The ongoing work is to involve quantization errors using multichannel audio coding methods in order to model the digital WFS method. It will be also necessary to validate the discrete model with real data taking into account the impulse response of the room for perceptual testing.

7. ACKNOWLEDGEMENTS

This work was supported by ISONAR Sound Research Workshop on Radio and Research Department, both at Universidad de San Martin de Porres, Lima, Peru.

8. REFERENCES

[1] A. Berkhout, "A holographic approach to acoustic control," in Journal of the Audio Engineering Society, vol. 36, no. 12, pp. 977-995, December 1988.

[2] A. Berkhout, D. de Vries and P. Vogel, "Acoustic control by wave field synthesis," in Journal of the Acoustic Society of America, vol. 93, no. 5, pp. 2664-2778, May 1993.

[3] D. de Vries, Wave Field Synthesis, Audio Engineering Society Monograph, April 2009.

[4] S. Spors, J. Ahrens and R. Rabenstein, "The theory of wave field synthesis revisited," in 124th Audio Engineering Society Convention, Amsterdam, The Netherlands, May 2008.

[5] S. Yon, M. Tanter and M. Fink, "Sound focusing in rooms: The time-reversal approach," in Journal of the Acoustic Society of America, vol. 113, no. 3, pp. 1533-1543, March 2003.

[6] S. Yon, M. Tanter and M. Fink, "Sound focusing in rooms. II. The spatio-temporal inverse filter," in Journal of the Acoustic Society of America, vol. 114, no. 6, pp. 3044-3052, December 2003.

[7] S. Spors, H. Wierstorf, M. Geier and J. Ahrens, "Physical and perceptual properties of focused sources in wave field synthesis," in 127th Audio Engineering Society Convention, New York, USA, October 2009.

[8] J. Ahrens and S. Spors, "Notes on rendering of focused directional sound sources in wave field synthesis," in 34rd German Annual Conference on Acoustics, Dresden, Germany, March 2008.

[9] P. Morse and K. Ingard, Theoretical acoustics, Princeton: Princeton University Press, 1986.

[10] M. Al-alaoui, "Novel digital integrator and differentiator," in Electronics letters, vol. 29, pp. 376-378, 1993.

[11] M. Al-alaoui, "Al-alaoui operator and the new transformation polynomials for discretization of analogue systems," in Electronic Engineering, Springer-Verlag, vol. 90, pp. 455-467, 2008.

[12] Oldham and J. Spanier, The fractional calculus, Academic Press, New York, USA, 1974.

[13] R. Barbosa, J. Tenreiro Machado and I. Ferreira, "Pole-zero approximations of digital fractional-order integrators and differentiators using signal modeling techniques," in Proceedings of the 16th IFAC World Congress, Prague, Czech Republic, July 2005.

[14] R. Barbosa and J. Tenreiro Machado, "Implementation of discrete-time fractional-order controllers based on LS aproximations," in Acta Polytechnica Hungarica, vol. 3, no. 4, pp. 5-22, 2006.

[15] T. Laakso, V. Välimäki, M. Karjalainen and U. Laine, "Splitting the unit delay: Tools for fractional delay filter design," IEEE Signal Processing Magazine, vol. 13, no. 1, pp. 30-60, January 1996.

[16] V. Välimäki and T. Laakso, "Principles of fractional delay filters," IEEE International Conference on Acoustics, Speech, and Signal Processing (ICASSP'00), Istanbul, Turkey, 5-9 June 2000.

[17] Pure Data: http://www.pure-data.org

[18] Lima Sonora: http://www.limasonora.com